A Family of α-Amino Acid Salicylaldiminates Incorporating the Binuclear $V_2O_3^{3+}$ Core: Electrosynthesis, Structure, and Metal Valence

Sujit Mondal, Prasanta Ghosh, and Animesh Chakravorty*

Department of Inorganic Chemistry, Indian Association for the Cultivation of Science, Calcutta 700 032, India

Received June 5, 1996[⊗]

The green title complexes of the type $Et_4N[V_2O_3(L\text{-Asal})_2]$ have been synthesized in nearly quantitative yields by one-electron electroreduction (at 0.2 V vs SCE) of $V_2O_3(L\text{-Asal})_2$ in dichloromethane solution containing tetraethylammonium perchlorate. Here L-Asal^{2-} is the deprotonated salicylaldimine of L-alanine (A = al), L-valine (A = va), or L-phenylalanine (A = pa). Electronic and IR spectra as well as metal reduction potentials ($E_{1/2} \sim$ 0.4 V vs SCE) of the complexes are reported. In $Et_4N[V_2O_3(L\text{-alsal})_2]\cdot$MeCN both the metal atoms have distorted square pyramidal geometry but the metrical differences between the two are considerable. The relative disposition of the two terminal V=O groups in the complex is intermediate between cis and trans. The V−O−V angle and V···V distance are 113.2(3)° and 3.067(3) Å, respectively. The two V−O lengths in the V−O−V bridge are very unequal, 1.768(6) and 1.905(7) Å, corresponding to a $V^{V}-O-V^{IV}$ description. Valence localization is consistent with the ^{51}V hyperfine structure of the axial EPR spectra ($3d_{xy}^1$ ground state) of the whole family of solid complexes: $s = {}^1/_2$; $g_{\|} \sim 1.95$, $g_{\perp} \sim 1.98$, $A_{\|} \sim 180$ G, and $A_{\perp} \sim 67$ G at 300 K. The spectra in frozen (77 K) dichloromethane solution are essentially the same. On the other hand, isotropic room temperature solution spectra of the family have 15 hyperfine lines ($g_{iso} \sim 1.97$; $A_{iso} \sim 51$ G) revealing that the unpaired electron and hence the metal valence are delocalized over both metal atoms on the X-band EPR time scale. The present results are compared with those of the few other $V_2O_3^{3+}$ complexes known revealing certain patterns. Crystal data for the $Et_4N[V_2O_3(L\text{-alsal})_2]\cdot$MeCN complex are as follows: chemical formula, $C_{30}H_{41}N_4O_9V_2$; crystal system, orthorhombic; space group, $P2_12_12_1$; $a = 9.797(5)$ Å, $b = 12.854(6)$ Å, $c = 27.550(11)$ Å; $Z = 4$.

Introduction

The tricationic trioxodivanadium core, $[OVOVO]^{3+}$, incorporating a formal $[V^{V}, V^{IV}]$ pair, is in principle a model binuclear mixed-valence system of the $[3d^0, 3d^1]$ type. It is expected to behave as a simple [$s = {}^1/_2$) EPR-active paramagnet whose ^{51}V (99.75%, $I = {}^7/_2$) hyperfine signature could disclose the locale of the electron and hence the state of metal oxidation. Studies on $V_2O_3^{3+}$ species have however been limited by the paucity of authentic complexes.[1−6] This has prompted us to initiate research in this area as a part of our program on oxovanadium chemistry.[5,7−9] At this stage our activity is primarily directed toward synthesis and structural characterization of new $V_2O_3^{3+}$ species. The longer term objective is to seek generalizations and correlations interlinking solid state structural parameters, solution properties, and valence mixing.

Herein we report the first example of a high-yield electrosynthetic procedure for preparing $V_2O_3^{3+}$ complexes. A family of the type $Et_4N[V_2O_3(L\text{-Asal})_2]$ has been isolated where L-Asal^{2-} is a chiral dianionic O,N,O-coordinating tridentate ligand (see below). The X-ray structure of one representative complex has been determined, revealing the presence of an unsymmetrical $V_2O_3^{3+}$ core. The status of metal valence in rigid and fluid matrices is scrutinized in terms of bond parameters and ^{51}V hyperfine data.

Results and Discussion

A. Electrosynthesis and Characterization. Salicylaldimines of L-alanine, L-valine, and L-phenylalanine are used as ligands (**1**; general abbreviation L-H_2Asal) in this work. It was

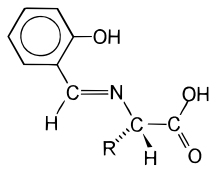

R = CH_3 L-H_2alsal
R = iPr L-H_2vasal
R = CH_2Ph L-H_2pasal

1

recently demonstrated in this laboratory that certain $V_2O_3^{3+}$ complexes can be generated in solution by constant potential electroreduction of the corresponding $V^{V}{}_2O_3^{4+}$ congeners.[5]

[⊗] Abstract published in *Advance ACS Abstracts,* November 1, 1996.

(1) Nishizawa, M.; Hirotsu, K.; Ooi, S.; Saito, K. *J. Chem. Soc., Chem. Commun.* **1979**, 707.
(2) (a) Kojima, A.; Okazaki, K.; Ooi, S.; Saito, K. *Inorg. Chem.* **1983**, *22*, 1168. (b) Okazaki, K.; Saito, K. *Bull. Chem. Soc. Jpn.* **1982**, *55*, 785.
(3) (a) Launay, J.; Jeannin, Y.; Daoudi, M. *Inorg. Chem.* **1985**, *24*, 1052. (b) Babonneau, F.; Sanchez, C.; Livage, J.; Launay, J. P.; Daoudi, M.; Jeannin, Y. *Nouv. J. Chim.* **1982**, *6*, 353.
(4) Pessoa, J. C.; L. Silva, J. A.; Vieira, A. L.; Vilas-Boas, L.; O'Brien, P.; Thornton, P. *J. Chem. Soc., Dalton Trans.* **1992**, 1745.
(5) (a) Dutta, S.; Basu, P.; Chakravorty, A. *Inorg. Chem.* **1993**, *32*, 5343. (b) Chakravarty, J.; Dutta, S.; Chakravorty, A. *J. Chem. Soc., Dalton Trans.* **1993**, 2857.
(6) Riechel, T. L.; Sawyer, D. T. *Inorg. Chem.* **1975**, *14*, 1869.
(7) (a) Chakravarty, J.; Dutta, S.; Chandra, S. K.; Basu, P.; Chakravorty, A. *Inorg. Chem.* **1993**, *32*, 4249. (b) Chakravarty, J.; Dutta, S.; Chakravorty, A. *J. Chem. Soc., Chem. Commun.* **1993**, 1091. (c) Chakravarty, J.; Dutta, S.; Dey, A.; Chakravorty, A. *J. Chem. Soc., Dalton Trans.* **1994**, 557.
(8) (a) Mondal, S.; Dutta, S.; Chakravorty, A. *J. Chem. Soc., Dalton Trans.* **1995**, 1115. (b) Mondal, S.; Rath, S. P.; Dutta, S.; Chakravorty, A. *J. Chem. Soc., Dalton Trans.,* in press. (c) Mondal, S.; Ghosh, P.; Chakravorty, A. *Indian J. Chem.* **1996**, *35A*, 171.
(9) (a) Basu, P.; Pal, S.; Chakravorty, A. *J. Chem. Soc., Dalton Trans.* **1991**, 3217. (b) Dutta, S.; Mondal, S.; Chakravorty, A. *Polyhedron* **1995**, *14*, 1163.

S0020-1669(96)00671-4 CCC: $14.00

Table 1. Selected Characterization Data of $Et_4N[V_2O_3(L\text{-}Asal)_2]$

Asal	μ_{eff}, μ_B	IR data[a], cm^{-1} VO	IR data[a], cm^{-1} $-CO_2$	UV−vis[b] λ_{max}, nm(ϵ, M^{-1} cm^{-1})	$E_{1/2}$[b−d], V (ΔE_p,[e] mV)
alsal	1.69	985, 760	1660, 1620, 1330	925 (180); 575 (220); 360 (4420)	0.44 (80)
vasal	1.70	980, 770	1650, 1620, 1320	935 (190); 575 (310); 360 (3820)	0.44 (120)
pasal	1.68	970, 760	1660, 1620, 1330	915 (240); 560 (440); 360 (5720)	0.46 (110)

[a] In KBr disks. [b] In CH_2Cl_2. [c] At a platinum electrode; supporting electrolyte, tetraethylammonium perchlorate (TEAP; 0.1 M); scan rate, 50 mV s^{-1}; reference electrode, SCE; solute concentration, $\sim 10^{-3}$ M. [d] $E_{1/2}$ is calculated as the average of anodic (E_{pa}) and cathodic (E_{pc}) peak potentials. [e] $\Delta E_p = E_{pa} - E_{pc}$.

We have now succeeded in utilizing the electrochemical procedure for the practical synthesis, eq 1, of green $Et_4N[V_2O_3$-

$$V^V{}_2O_3(L\text{-}Asal)_2 + e^- + Et_4N^+ \xrightarrow[CH_2Cl_2]{0.2\ V} Et_4N[V_2O_3(L\text{-}Asal)_2] \quad (1)$$

$(L\text{-}Asal)_2]$ in virtually quantitative yield. The $V^V{}_2O_3(L\text{-}Asal)_2$ precursor[10,11] prepared from VO(OMe)(HOMe)(L-Asal)[9b,10,12] displayed a quasireversible cyclic voltammetric response near 0.4 V vs SCE in dichloromethane solution. The response was logically assigned to the $V_2O_3(L\text{-}Asal)_2-V_2O_3(L\text{-}Asal)_2^-$ couple, and on this basis the constant working potential for the electrosynthesis was set at 0.2 V vs SCE. The cyclic voltammogram of $Et_4N[V_2O_3(L\text{-}Asal)_2]$ (initial scan anodic) was the same as that of the precursor (initial scan cathodic) as expected. The electrosynthetic method developed here is new in $V_2O_3{}^{3+}$ chemistry. The few reported $V_2O_3{}^{3+}$ complexes have been prepared either by reaction of preformed VO^{2+} and $VO_2{}^+$ complexes[1,3,6] or by the oxidation of VO^{2+} chelates.[2,4]

Selected characterization data of the $Et_4N(V_2O_3(L\text{-}Asal)_2]$ complexes are listed in Table 1. Solution conductivity corresponds to 1:1 electrolytic behavior, (Λ, 130−135 Ω^{-1} cm^2 mol^{-1} in MeCN). Magnetic moments are consistent with the presence of one unpaired electron ($s = {}^1/_2$); EPR spectra will be treated in a later section. In IR, terminal and bridging VO stretching modes are observed near 980 and 760 cm^{-1}, respectively. Monodentate carboxyl coordination is consistent with the presence of one symmetric ($\sim$1330 cm^{-1}) and two asymmetric ($\sim$1660 and $\sim$1620 cm^{-1}) stretching modes.[13] In electronic spectra a band of moderate intensity occurs near 930 nm. Absorption in this region is a characteristic feature of the $V_2O_3{}^{3+}$ core.[1−3,5]

B. Structure. The L-alsal^{2-} complex afforded good crystals as the solvate $Et_4N[V_2O_3(L\text{-}alsal)_2]\cdot MeCN$. The lattice consist of discrete cations, anions and MeCN molecules which are not bonded to the metal atom in any way. A view of the binuclear anion is shown in Figure 1, and selected bond parameters are listed in Table 2.

a. Geometrical Features. Both the metal atoms have distorted square pyramidal geometry[14] of coordination type

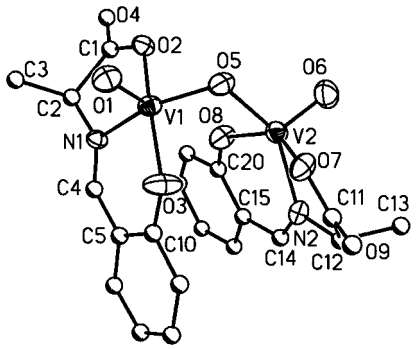

Figure 1. Perspective view and atom-labeling scheme for the complete anion in $Et_4N[V_2O_3(L\text{-}alsal)_2]\cdot MeCN$.

Table 2. Selected Bond Distances (Å) and Angles (deg) for $[Et_4N][V_2O_3(L\text{-}alsal)_2]\cdot MeCN$

Distances			
V1−O1	1.591(7)	V2−O6	1.583(9)
V1−O2	1.969(6)	V2−O7	1.964(8)
V1−O3	1.890(9)	V2−O8	1.932(7)
V1−N1	2.106(7)	V2−N2	2.075(8)
V1−O5	1.768(6)	V2−O5	1.905(7)
C4−N1	1.297(11)	C14−N2	1.253(14)
V1···V2	3.067(3)		
Angles			
O2−V1−O3	153.6(3)	O7−V2−O8	143.6(3)
N1−V1−O5	147.5(3)	N2−V2−O5	146.4(3)
O1−V1−O2	99.3(3)	O6−V2−O7	106.5(4)
O1−V1−O5	105.9(3)	O6−V2−O5	108.8(4)
O1−V1−O3	104.2(4)	O6−V2−O8	109.2(4)
O1−V1−N1	105.9(3)	O6−V2−N2	104.7(4)
O2−V1−N1	76.6(3)	O7−V2−N2	78.2(3)
O2−V1−O5	91.9(3)	O7−V2−O5	90.0(3)
O3−V1−O5	93.4(4)	O8−V2−O5	85.5(3)
O3−V1−N1	85.3(3)	O8−V2−N2	85.9(3)
V1−O5−V2	113.2(3)		

VO_4N. The two coordination pyramids are metrically distinct. Thus the V1 atom is displaced toward the terminal 01 atom by 0.46 Å from the mean plane of O2, O5, O3, and N1. The corresponding displacement of V2 toward the O6 atom from the plane of O7, O5, O8, and N2 is 0.59 Å. The L-alsal^{2-} ligand binds the metal in the O,N,O-tridentate meridional fashion. It is not planar but is constituted of two planar (mean deviation < 0.04 Å) segments, CCO_2 and NCC_6H_4O, intersecting along a N−C single bond (N1−C2 and N2−C12). The dihedral angle between the segments is 39.0° for the ligand attached to V1 and 27.9° for that attached to V2.

The signs of atomic coordinates of the $Et_4N[V_2O_3(L\text{-}alsal)_2]\cdot$ MeCN were made to conform to the *S*-configuration of the L-amino acid residue. Viewing any of the two metal centers down the unique V═O(terminal oxo) axis and setting the priority sequence O(bridging) > O(carboxylate) > O(phenolate) > N(azomethine) for the coordinated atoms, the absolute config-

(10) Nakajima, K.; Kojima, M.; Toriumi, K.; Saito, K.; Fujita, J. *Bull. Chem. Soc. Jpn.* **1989**, *62*, 760.

(11) Spectral data for $V_2O_3(L\text{-}Asal)_2$ precursors are as follows. VO stretching (cm^{-1}) in KBr disks: for $V_2O_3(L\text{-}alsal)_2$, 990, 760; for $V_2O_3(L\text{-}vasal)_2$, 990, 770; for $V_2O_3(L\text{-}pasal)_2$, 990, 765. UV−vis spectra λ_{max}, nm (ϵ, M^{-1} cm^{-1}) in CH_2Cl_2: for $V_2O_3(L\text{-}alsal)_2$ 560 (1230), 325 (13475); for $V_2O_3(L\text{-}vasal)_2$ 580 (1420), 340 (13460); and for $V_2O_3(L\text{-}pasal)_2$, 575 (1140), 340 (12880).

(12) (a) Fraústa da Silva, J. J. R.; Wooton, R.; Gillard, R. D. *J. Chem. Soc. A* **1970**, 3369. (b) Cavaco, I.; Pessoa, J. C.; Costa, D.; Duarte, M. T.; Gillard, R. D.; Matias, P. *J. Chem. Soc., Dalton Trans.* **1994**, 149.

(13) Kavanagh, B.; Steed, J. W.; Tocher, D. A. *J. Chem. Soc., Dalton Trans.* **1993**, 327.

(14) Description in terms of distorted trigonal bipyramidal geometry is not appropriate. Thus in the case of V1O4N, O2V1O3 is a poor axis since the angle at the metal is 154° and in the V1O1O5N1 base the angle at the metal between consecutive atom pairs are 106, 148, and 106°.

(15) Leigh, G. J. (Editor) *Nomenclature of Inorganic Chemistry*; Blackwell Scientific Publications: Oxford, England, 1990; p 186.

uration is found to be of the anticlockwise type[15] in the cases of both V1 and V2. Diastereoisomers with clockwise configuration of one or both metal atoms have not been observed. In the anticlockwise configuration the V1═O1 and C2−C3 bonds lie mutually endo to each other and the same applies to V2═O6 and C12−C13 bonds (Figure 1).

b. The $V_2O_3^{3+}$ Core. The relative disposition of the two V═O groups in V_2O_3(L-alsal)$_2^-$ is intermediate between cis and trans, the O1═V1···V$_2$═O6 torsion angle being 83.7°. The two L-alsal^{2-} ligands thus occur in nearly orthogonal domains. This ensures lack of steric crowding of the ligands even though the bridge angle V1−O5−V2 is only 113.2(3)°. The V1···V2 distance is 3.067(3) Å. The σ-hybridization of the O5 atom evidently lie between sp^2 and sp^3. The bridge angle in our complex is much smaller than those so far reported for $V_2O_3^{3+}$ complexes (146.6(2)−180°).[1−4] The relative disposition of the V═O groups noted above is also unique. In reported complexes the disposition is either exactly[1] or nearly[2a,3a] trans or nearly cis.[4]

The two sides of the VOV bridge are very unequal: V1−O5, 1.768(6) Å, and V2−O5, 1.905(7) Å. In the synthetic precursor $V^V_2O_3$(L-alsal)$_2$ the bridging V−O lengths lie[10] in the range 1.79−1.82 Å, which can be compared with the V1−O5 length in our complex. On the other hand in $V^{IV}O(OH_2)$(L-alsal)[16] the V−OH$_2$ length is 2.003(3) Å (compare with V2−O5 length in our complex). These correlations suggest that the V1 and V2 atoms are V^V and V^{IV} respectively. The V1−N1 bond, 2.106(7) Å, is longer than the V2−N2 bond, 2.075(8) Å, consistent with the stronger trans influence of the shorter V1−O5 bond.

The V1═O1 and V2═O6 lengths are equal within experimental error. Quite generally bonds to terminal oxo atoms are full double bonds for both V^V and V^{IV} and their lengths are known to be relatively insensitive to the metal oxidation state lying within ±0.03 Å of 1.58 Å.[7a] But the V^V═O and V^{IV}═O motifs differ in one important respect: the former seeks additional double bonding (π-bonding) with other donor sites, the latter being relatively ineffective in this respect. The shortness of the V1−O5 bond is ascribed to such partial double bond character. In the simplified description **2** (arbitrary

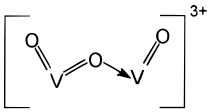

2

conformation), the $V_2O_3^{3+}$ core is viewed as a coordination complex between the donor $V^VO_2^+$ and the acceptor $V^{IV}O^{2+}$. The unequal lengths of the V−O(phenolic) bonds are also noteworthy: V1−O3, 1.890(9) Å, and V2−O8, 1.932(7) Å. Partial V^V−O(phenolic) double bonding has been documented.[5,8]

The structures of just four other $V_2O_3^{3+}$ complexes are known: $V_2O_3(nta)_2^{3-}$,[1] V_2O_3(*S*-peida)$_2^-$,[2a] $V_2O_3(pmida)_2^-$ [3a] (ligands as in **3**), and V_2O_3(DL-salser)$_2^-$ [4] where DL-salser^{2-} is

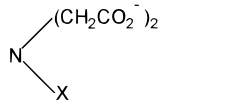

	X
nta^{3-}	$CH_2CO_2^-$
pmida^{2-}	$CH_2C_6H_4N(\alpha)$
S-peida^{2-}	*S*-$CHMeC_6H_4N(\alpha)$

3

akin to **1** being the salicylaldimine of DL-serine. In the first three structures the VO^{b}V fragment is linear or nearly so (175−180°)[17] corresponding to sp σ-hybridization of O^b, the bridging oxo atom. This ensures maximum V···V separation (∼3.62 Å)[17] and hence minimum steric interference between the pseudo-octahedral metal coordination spheres. In V_2O_3(DL-salser)$_2^-$ the metal atoms are pentacoordinated, the steric situation is more relaxed and the bridge is nonlinear (∼147°)[17], the O^b σ-hybridization being intermediate between sp and sp^2. Finally in our complex V_2O_3(L-alsal)$_2^-$, also pentacoordinated, we have more severe bridge nonlinearity associated with O^b hybridization between sp^2 and sp^3. In all cases except centrosymmetric $V_2O_3(nta)_2^{3-}$,[1] the two V−O^b bonds are unequal.[2a,3a,4,17]

It is particularly instructive to compare our complex V_2O_3(L-alsal)$_2^-$ with V_2O_3(*S*-peida)$_2^-$,[2a] both being chiral. They differ widely in metal coordination geometry (square pyramid vs octahedron) and O^b σ-hybridization (sp^2−sp^3 vs ∼sp). Yet the V−O^b bonds (1.77, 1.91 Å vs[17] 1.76, 1.88 Å) are unequal to very similar extents. The rationale is that the V−O^b length inequality originates (*vide supra*) from π-bonding primarily at the V^V site. Such bonding would evidently persist irrespective of O^b hybridization as long as one O^b orbital is at least partially available for π-bonding with V^V. In spite of the small size (five only) of the structural sample, a rudimentary pattern of $V_2O_3^{3+}$ chemistry is silhouetted in the above observations. First, the σ-hybridization of O^b and hence the bridge angle and V···V separations are subject to major control by the mutual steric requirements of the metal coordination spheres rather than by any basic electronic need. Second, unequal V−O^b bonds and hence the tendency toward valence localization (V^V, V^{IV}) is the more common situation irrespective of the σ-hybridization of O^b.

C. EPR Spectra. The $Et_4N[V_2O_3$(L-Asal)$_2]$ complexes are EPR-active in pure solid form as well as in dichloromethane solution (300 K, 77 K). Resonance parameters are listed in Table 3 and representative spectra are shown in Figure 2.

Powders of the pure complexes display well-resolved axial spectra both at room temperature and at 77 K. The hyperfine structure corresponds to the coupling of the unpaired electron to a single ^{51}V ($I = {}^7/_2$) atom (Figure 2). The order ($g_{||} < g_\perp$ and $A_{||} \gg A_\perp$) and magnitude (Table 3) of resonance parameters are consistent with a oxovanadium(IV) site of compressed d_{xy}^1 configuration.[7,8a,18] The spectra of the pure complexes are surprisingly sharp for an undiluted paramagnetic solid. The large Et_4N^+ cations ensure that the binuclear anions and hence the oxovanadium(IV) sites are well spaced in the lattice (minimum V^{IV}···V^{IV} separation in $Et_4N[V_2O_3$(L-alsal)$_2]$·MeCN is 7.74 Å), diminishing mutual line-broadening interactions.

The spectra of the complexes in frozen (77 K) dichloromethane solutions are very similar to those of powdered solids (Table 3, Figure 2). On the other hand, isotropic room temperature (300 K) solution spectra reveal the presence of 15 lines (Figure 2) arranged in a more or less symmetrical manner showing that the unpaired electron is coupled to both the ^{51}V

(16) Hämäläinen, R.; Turpeinen, U.; Ahlgreen, M. *Acta. Crystallogr.* **1985**, *C41*, 1726.

(17) The V−O^b−V angle (deg), V···V distance (Å), O═V···V═O torsion angle (deg), and V−O^b distances (Å) are as follows: for $(NH_4)_3[V_2O_3(nta)_2]\cdot 3H_2O$[1]; 180, 3.620(1), 180, and 1.810(1), 1.810(1); for Na-$[V_2O_3$(*S*-peida)$_2]\cdot NaClO_4\cdot H_2O$,[2a] 179.5(3), 3.673(2), 164.3(2), and 1.763(4), 1.875(4); for $H[V_2O_3(pmida)_2]\cdot 4H_2O$[3a], 175.3(7), 3.617(2), 178.9(3), and 1.79(2), 1.82(2); for $Na[V_2O_3$(DL-salser)$_2]\cdot 5H_2O$[4], 146.6-(2), 3.467(2), 10.5(3), and 1.754(6), 1.866(5). The parameters were calculated (where not reported) from the available atomic coordinates. In the case of V_2O_3(DL-salser)$_2^-$ the reported[4] torsion angle is 11.6° but we have calculated it to be 10.5°.

(18) (a) Cornman, C. R.; Kampf, J.; Lah, M. S.; Pecoraro, V. L. *Inorg. Chem.* **1992**, *31*, 2035. (b) Hausan, G. R.; Kabanos, T. A.; Keramidas, A. D.; Mentzafos, D.; Terzis, A. *Inorg. Chem.* **1992**, *31*, 2587.

Table 3. X-Band EPR Data for $Et_4N[V_2O_3(L\text{-}Asal)_2]$

Asal	matrix	g_{iso}	A_{iso}, G	$g_{\|}$	$g_{\perp}$	g_{av}[a]	$A_{\|}$, G	$A_{\perp}$, G	A_{av},[b] G
alsal	CH_2Cl_2, 300 K	1.973	51.4						
	CH_2Cl_2, 77 K			1.951	1.982	1.972	177.9	63.4	101.5
	solid, 300 K			1.950	1.982	1.971	180.0	67.1	104.8
	solid, 77 K			1.950	1.985	1.973	182.8	67.1	105.6
vasal	CH_2Cl_2, 300 K	1.968	51.4						
	CH_2Cl_2, 77 K			1.952	1.981	1.971	177.9	61.4	100.2
	solid, 300 K			1.948	1.981	1.970	183.6	68.5	106.8
	solid, 77 K			1.951	1.986	1.974	181.4	67.1	105.2
pasal	CH_2Cl_2, 300 K	1.977	51.4						
	CH_2Cl_2, 77 K			1.950	1.978	1.969	178.6	62.1	100.9
	solid, 300 K			1.944	1.976	1.965	182.8	67.8	106.2
	solid, 77 K			1.952	1.978	1.969	180.7	69.0	106.2

[a] $g_{av} = {}^1/_3[2g_{\perp} + g_{\|}]$. [b] $A_{av} = {}^1/_3[2A_{\perp} + A_{\|}]$.

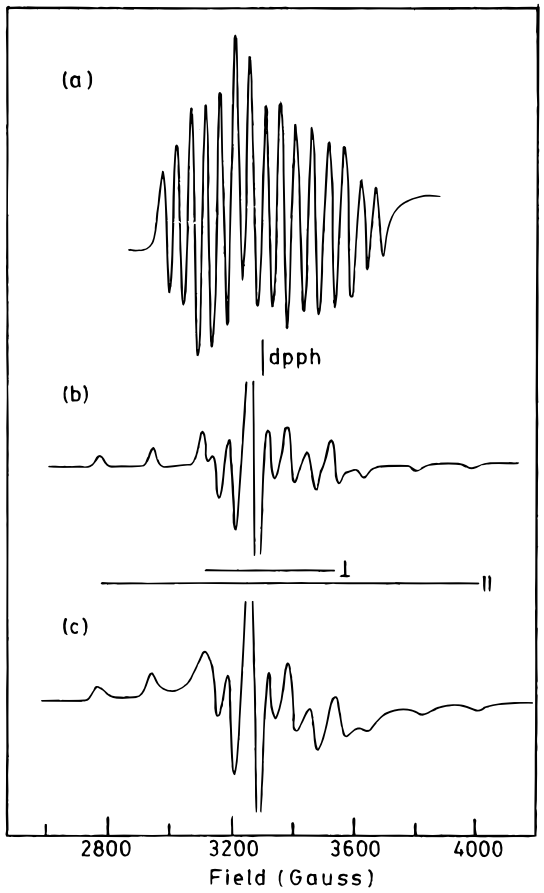

Figure 2. EPR spectra at X-band of $Et_4N[V_2O_3(L\text{-alsal})_2]$: (a) CH_2Cl_2, 300 K; (b) CH_2Cl_2, 77 K; (c) powdered solid, 300 K. Instrument settings: power, 30 dB; modulation, 100 kHz; sweep center, 3200 G; sweep width, 2000 G; sweep time, 240 s.

nuclei. Coupling to just one nucleus would have given rise to eight isotropic lines only. The spectral changes between fluid and rigid matrices are entirely reversible, Scheme 1. Attempts were made to identify the possible transition from 15 lines to eight lines in fluid solutions by varying the temperature (300−77 K).[5,19] Upon cooling, the spectra became progressively broad, and no coalescence temperature could be reliably defined.[20] The anisotropic frozen solution axial spectrum became recognizable just below the freezing point of the dichloromethane solvent (176 K).

Scheme 1

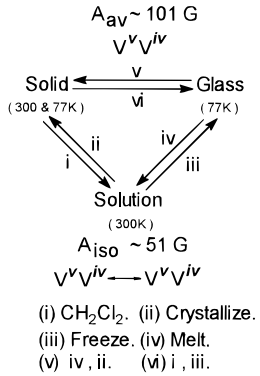

D. Metal Valence in Rigid and Fluid Matrices. Taken collectively, the X-ray and EPR results demonstrate that metal valences are localized uniquely in a $[V^V, V^{IV}]$ potential energy trap (class I sense[21]) in $Et_4N[V_2O_3(L\text{-Asal})_2]$ when the lattice is rigid—be it the pure solid state or be it the frozen solution state. Spectral parameters (Table 3) of the rigid states correlate with those of fluid solutions as in eq 2. In such solutions the unpaired

$$g_{av} \approx g_{iso}; \quad A_{av} \approx 2A_{iso} \tag{2}$$

electron is thus[5,22] more or less equally delocalized over the two metal atoms at least on the X-band EPR time-scale. This can be conveniently depicted as $V^V,V^{IV} \leftrightarrow V^{IV},V^V$ (class II or III).[21] The class placement cannot be made more specific at present.

The presence of unequal $V-O^b$ bonds in the other reported complexes[2a,3a,4,17] suggest that valence localization in the solid state may be a common thing among $V_2O_3^{3+}$ complexes. Unfortunately well-resolved rigid lattice EPR data are not available for any of these cases.[3a] Fluid solution EPR data have however been reported in a number of cases and all of these have 15-line spectra with A_{iso} in the range 50−53 G.[1,3a,5] Valence delocalization on the EPR time scale may very well be a rather general feature of $V_2O_3^{3+}$ complexes in fluid solutions.

(19) (a) Gagne, R. R.; Koval, C. A.; Smith, T. J.; Cimolino, M. C. *J. Am. Chem. Soc.* **1979**, *101*, 4571. (b) Long, R. C.; Hendrickson, D. N. *J. Am. Chem. Soc.* **1983**, *105*, 1513.

(20) At the coalescence temperature the life time of the localized state would approximately equal to $1/\sqrt{2}\pi A_{iso}$ or 10^{-9} s. If the coalescence temperature is assumed to lie a few degrees above the freezing point of the dichloromethane solvent (176 K), e.g. 180 K, the activation energy and rate constant of the localized → delocalized transformation can be computed as ~3 kcal mol^{-1} and ~10^{10} s^{-1} (at 300 K) respectively.[5,19] However the very broad nature of resonances at low temperature makes such an analysis untenable.

(21) (a) Robin, M. B.; Day, P. *Adv. Inorg. Chem.* **1967**, *10*, 247. (b) Wong, K. Y.; Schatz, P. N. *Prog. Inorg. Chem.* **1981**, *28*, 369.

(22) (a) Wertz, J. E.; Bolton, J. R. *Electron Spin Resonance*; McGraw-Hill: New York, 1972; p 210. (b) Pilbrow, J. R. *Transition Ion Electron Paramagnetic Resonance*; Clarendon Press: Oxford, U.K., 1990; p 339.

Concluding Remarks

The main findings of this work will now be recapitulated. Electroreduction of the $V_2O_3^{4+}$ core to $V_2O_3^{3+}$ has been successfully utilized for practical synthesis of the $Et_4N[V_2O_3(L\text{-Asal})_2]$ family in nearly quantitative yield. In $Et_4N[V_2O_3(L\text{-alsal})_2]\cdot MeCN$, the V−O−V angle is ∼113°, the smallest value so far observed among $V_2O_3^{3+}$ complexes. Examination of known structures indicates that the conformation of the $V_2O_3^{3+}$ core is inherently flexible easily adjusting to the steric needs of metal coordination spheres.

The X-ray (very unequal $V-O^b$ lengths) and EPR (^{51}V hyperfine structure) results demonstrate that rigid lattices (pure solid, frozen solution) enforce valence localization in $V_2O_3(L\text{-Asal})_2^-$. On the other hand, fluid solutions promote valence delocalization on the EPR time scale. Such delocalization appears to be a common feature of most $V_2O_3^{3+}$ complexes so far examined in solution. The nature of the structural change between solid and liquid solution phases are not clear at present, but the flexibility of the $V_2O_3^{3+}$ core can be expected to be most expressed in the fluid-solvated situation. This could be a crucial factor in bringing about effective valence mixing in fluid solution. Further work is in progress.

Experimental Section

Materials. The starting VO(OMe)(HOMe)(L-Asal) complexes were prepared by reported methods.[9b,10,11] Electrochemical grade dichloromethane, methanol, acetonitrile, and tetraethylammonium perchlorate (TEAP) were obtained as before.[23] All other chemicals and solvents were of analytical grade and used as received.

Physical Measurement. Infrared spectra were recorded on a Perkin-Elmer 783 spectrometer, and a Hitachi 330 spectrometer was used to obtain electronic spectra. EPR spectra were obtained at X-band frequencies on a Varian E-109C spectrometer equipped with a gas-flow temperature controller for variable-temperature studies. Spectra at 77 K were collected using a quartz dewar. The calibrant was DPPH ($g = 2.0037$). Magnetic susceptibility was measured using a PAR 155 vibrating-sample magnetometer fitted with a Walker Scientific L75 FBAL magnet. Microanalytical (C, H, N) data were obtained from a Perkin-Elmer 240C elemental analyzer. All electrochemical measurements were performed under nitrogen atmosphere using a PAR 370−4 electrochemistry system as reported before.[24] All potentials reported in this work are uncorrected for junction contribution. Solution (∼10^{-3} M) electrical conductivities were measured with the help of a Philips PR 9500 bridge.

Preparation of Complexes. The complexes reported in this work were prepared by the one-electron electroreduction of the $V_2O_3(L\text{-Asal})_2$ precursors of which $V_2O_3(L\text{-alsal})_2$ is already known.[10] The other two were prepared by using the same general method, and details are given below for one case.

(μ-Oxo)bis[(*N*-salicylidene-L-phenylalaninato)oxovanadium(V)], V_2O_3(L-pasal)$_2$. A 0.20 g (0.50 m mol) sample of VO(OMe)(HOMe)(L-pasal) was dissolved in 20 mL of dichloromethane by stirring in air. The resulting dark blue solution upon standing in air yielded a crystalline solid. It was filtered and dried in vacuum. Yield: 0.33 g (96%). Anal. Calcd for $C_{32}H_{26}N_2O_9V_2$: C, 56.14; H, 3.80; N, 4.09. Found: C, 56.05; H, 3.98; N, 4.09.

The complex $V_2O_3(L\text{-vasal})_2$ was prepared similarly in 94% yield. Anal. Calcd for $C_{24}H_{26}N_2O_9V_2$: C, 48.98; H, 4.42; N, 4.76. Found: C, 48.87; H, 4.47; N, 4.67.

Table 4. Crystallographic Data for $Et_4N[V_2O_3(L\text{-alsal})_2]\cdot MeCN$

chemical formula	$C_{30}H_{41}N_4O_9V_2$	T, °C	22
fw	703.5	λ, Å	0.710 73
space group	$P2_12_12_1$	ρ_{obsd}, g cm^{-3}	1.350
a, Å	9.797(5)	ρ_{calcd}, g cm^{-3}	1.347
b, Å	12.854(6)	μ, cm^{-1}	5.93
c, Å	27.550(11)	R,[a] %	5.25
V, Å^3	3469(3)	R_w,[b] %	5.56
Z	4		

[a] $R = \sum||F_o| - |F_c||/\sum|F_o|$. [b] $R_w = [\sum w(|F_o| - |F_c|)^2/\sum w|F_o|^2]^{1/2}$; $w^{-1} = \sigma^2(|F_o|) + g|F_o|^2$; $g = 0.0001$.

Tetraethylammonium (μ-Oxo)bis[(*N*-salicylidene-L-alaninato)oxovanadate], $Et_4N[V_2O_3$(L-alsal)$_2]$. A solution of 0.10 g (0.19 mmol) of $V_2O_3(L\text{-alsal})_2$ and 0.043 g (0.19 mmol) of TEAP in 30 mL of dry dichloromethane was reduced coulometrically at a constant potential of 0.2 V vs SCE in nitrogen atmosphere. As the reduction proceeded, the color of the solution changed from blue to green. Electrolysis stopped when 17.14 C had passed. The calculated one-electron Coulomb count is 18.22. The resulting green solution upon evaporation to dryness afforded $Et_4N[V_2O_3(L\text{-alsal})_2]$. Yield: 0.122 g (97%). Anal. Calcd for $C_{28}H_{38}N_3O_9V_2$: C, 50.75; H, 5.74; N, 6.34. Found: C, 50.60; H, 5.82; N, 6.32.

The other two mixed-valence complexes were prepared similarly in 95−97% yield. Anal. Calcd for $Et_4N[V_2O_3(L\text{-vasal})_2]$, $C_{32}H_{46}N_3O_9V_2$: C, 53.48; H, 6.41; N, 5.85. Found: C, 53.37; H, 6.35; N, 5.78. Anal. Calcd for $Et_4N[V_2O_3(L\text{-pasal})_2]$, $C_{40}H_{46}N_3O_9V_2$: C, 58.97; H, 5.65; N, 5.16. Found: C, 58.87; H, 5.77; N, 5.20.

Single Crystals of $Et_4N[V_2O_3$(L-alsal)$_2]\cdot MeCN$. These were grown by electrosynthesizing the complex in dry MeCN (instead of CH_2Cl_2) and crystallizing by slow evaporation under reduced pressure. Anal. Calcd for $C_{30}H_{41}N_4O_9V_2$: C, 51.20; H, 5.83; N, 7.96. Found: C, 50.84; H, 5.92; N, 7.89.

X-ray Structure Determination. The cell parameters of a $Et_4N[V_2O_3(L\text{-alsal})_2]\cdot MeCN$ crystal (0.3 × 0.4 × 0.3 mm^3) were determined by a least-squares fit of 30 machine-centered reflections ($2\theta = 15-30°$). Data were collected by the ω-scan method in the range $3° \le 2\theta \le 50°$ on a Nicolet R3m/V four-circle diffractometer with graphite-monochromated Mo Kα radiation ($\lambda = 0.710\,73$ Å). Two check reflections measured after every 98 reflections showed no intensity reduction. Data were corrected for Lorentz−polarization effects, and empirical absorption correction was done on the basis of azimuthal scans of six reflections.[25] Total reflections collected, unique reflections, and used reflections for structure solution satisfying $I > 3\sigma(I)$ were 3586, 3481, and 1831 respectively. Systematic absences led to the identification of the space group as $P2_12_12_1$.

All calculations for data reduction, structure solution and refinement were done on a Micro VAXII computer with the programs of SHELXTL-PLUS.[26] The structure was solved by direct method and refined by a full-matrix least-squares procedure. All vanadium, oxygen, and nitrogen atoms were made anisotropic. The thermals parameter of the Et_4N^+ cation atoms were relatively high, and these were also made anisotropic. Hydrogen atoms were included in calculated positions with fixed U (=0.08 Å^2). The highest difference Fourier peak is 0.41 e/Å^3. Significant crystal data are listed in Table 4.

Acknowledgment. Financial support received from the Department of Science and Technology, and the Council of Scientific and Industrial Research, New Delhi, is acknowledged. Affiliation with the Jawaharlal Nehru Centre for Advanced Scientific Research, Bangalore, India, is acknowledged. We are thankful to Dr. S. Dutta for preliminary experiments.

Supporting Information Available: For $Et_4N[V_2O_3(L\text{-alsal})_2]\cdot MeCN$ tables of crystal data (Table S1), complete atomic coordinates (Table S2), bond distances (Table S3) and angles (Table S4), anisotropic thermal parameters (Table S5), and hydrogen atoms positional parameters (Table S6), (6 pages). Ordering information is given on any current masthead page.

IC960671R

(23) Dutta, D.; Mascharak, P. K.; Chakravorty, A. *Inorg. Chem.* **1981**, *20*, 1673.
(24) Chandra, S. K.; Basu, P.; Ray, D.; Pal, S.; Chakravorty, A. *Inorg. Chem.* **1990**, *29*, 2423.
(25) North, A. C. T.; Philips, D. C.; Mathews, F. S. *Acta Crystallogr., Sect. A* **1968**, *24*, 351.
(26) Sheldrick, G. M. *SHELXTL-PLUS 88, Structure Determination Software Programs*; Nicolet Instrument Corp.: Madison, WI, 1988.